SENSING-ASSISTED BEAM TRACKING IN V2I NETWORKS: EXTENDED TARGET CASE

Zhen Du[⋆†], *Fan Liu*[†], *Zenghui Zhang*[⋆]

[⋆] Shanghai Jiao Tong University, Shanghai 200240, China
[†] Southern University of Science and Technology, Shenzhen 518055, China
(Invited Paper)

ABSTRACT

A sensing-assisted predictive beamforming scheme for vehicle-to-infrastructure (V2I) communication is considered, which is built upon massive multi-input-multi-output (mMIMO) and millimeter wave (mmWave) techniques. In practical V2I networks, vehicles cannot be modeled as point targets in terms of the narrow beamwidth and high range resolution. Accordingly, the communication receiver (CR) may be beyond the beam even the vehicle is accurately tracked, which makes robust beam alignment and tracking challenging. We thus consider the extended target case, in which the beamwidth should be adjusted in real-time to cover the entire vehicle. Then an extended Kalman filtering (EKF) is presented to track the CR according to the resolved high-resolution geometry results. Finally, numerical results are provided to validate the effectiveness of the proposed approach.

***Index Terms*—** Beam tracking, ISAC, mmWave, EKF

1. INTRODUCTION

Vehicle-to-everthing (V2X) communication has been upgraded thanks to the application of the fifth-generation (5G) communication techniques, which brings the advantages of low-latency and large bandwidth [1]. Meanwhile, sensing capability has a great potential of enabling the accurate and robust vehicle tracking. Recent efforts have been taken to investigate the feasibility of integrated sensing and communication (ISAC) in V2X networks. In [2, 3], using mmWave ISAC signaling to align the mMIMO beamforming in V2I networks is proposed. The echo is collected for measuring the state parameters with matched-filtering, and then predicting the localization of vehilce to achieve beamforming. Compared to the conventional beam training [4, 5] or beam tracking [6, 7], advantages of the ISAC beam tracking are summarized as coordination gain plus integration gain [8, 9].

The aforementioned works are dedicated to handling point-like vehicles. The mMIMO antenna array yields the pencile-like beam, which demonstrates that the vehicle is unlikely to be entirely illuminated by the narrow beam, especially when it approaches the illuminator. On account of this reason, even the vehicle can be accurately tracked, however the communication rate may be poor because the communication receiver (CR) may not lie in the effective beamwidth. Besides, the large bandwidth arises the high range resolution, especially the mmWave signal has the bandwidth up to the order of GHz, indicating that the vehicle is distributed in multiple range cells. Therefore, the vehilce can be extended in both range and angle domain, so that the approaches discussed in [2, 3, 10] significantly degrade.

To cope with the above challenges, we propose a dynamic ISAC beam tracking in V2I networks for the extended target case. Since the rectangle geometry of extended target with multiple scatterers are resolved, coordinates of the CR can be inferred according to measurements of all scatterers. Subsequently, the beam tracking can be performed with the developed extended Kalman filtering (EKF) algorithm.

2. SYSTEM MODELING

Throughout this paper, the roadside unit (RSU) operates at the mmWave band and is equipped with mMIMO uniform linear array (ULA) which has $N_{t,n}$ transmit antennas and N_r receive antennas. Denote the angle, the distance and the velocity of the vehicle's CR relative to the RSU's array by $\phi(t)$, $d(t)$ and $v(t)$, respectively. All these motion parameters are defined in the region $t \in [0, T]$, with T being the maximum time duration of interest. We discretize T into several small time-slots with a length of ΔT. Further, denote the motion parameters at the nth epoch by ϕ_n, d_n and v_n, where $\phi_n = \phi(n\Delta T)$, $d_n = d(n\Delta T)$ and $v_n = v(n\Delta T)$, respectively.

2.1. Radar Signal Model

The scenario diagram is shown in Fig. 1. At the nth epoch, the RSU receives the echo contributed by the vehicle's K resolved scatterers with N_r receive antennas, expressed as

$$\mathbf{r}_n(t) = \kappa_n \sqrt{p_n} \sum_{k=1}^{K} \beta_{k,n} e^{j2\pi\mu_{k,n}t} \mathbf{b}\left(\theta_{k,n}\right) \mathbf{a}^H\left(\theta_{k,n}\right) \mathbf{f}_n \times s_n\left(t - \tau_{k,n}\right) + \mathbf{z}_r(t), \tag{1}$$

where $\mathbf{r}_n(t) \in \mathbb{C}^{N_r \times 1}$; $\kappa_n = \sqrt{N_{t,n} N_r}$ is the array gain factor; p_n denotes the transmitted power; $\mu_{k,n}$, $\beta_{k,n}$ and $\tau_{k,n}$

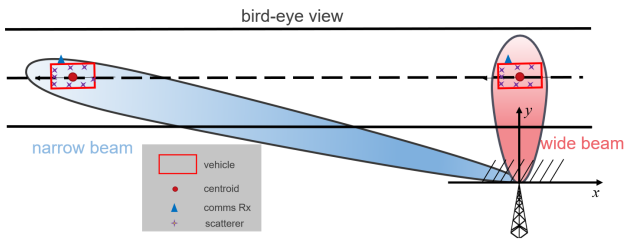

Fig. 1. ISAC-based beam tracking with dynamic beamwidth.

denote the Doppler frequency, the complex reflection coefficient and the round-trip delay of the kth scatterer at the nth epoch, respectively; $\mathbf{z}_n(t) \in \mathbb{C}^{N_r \times 1}$ represents the complex additive white Gaussian noise with zero mean and variance of σ^2, i.e., $\mathbf{z}_r(t) \sim \mathcal{CN}(\mathbf{0}_{N_r}, \sigma^2 \mathbf{I}_{N_r})$.

Besides, $\mathbf{a}_n(\theta)$ and $\mathbf{b}(\theta)$ are transmit and receive steering vectors of the RSU's ULA, in the forms of

$$\mathbf{a}(\theta) = \frac{1}{\sqrt{N_{t,n}}}[1, e^{-j\pi\cos\theta}, \cdots, e^{-j\pi(N_{t,n}-1)\cos\theta}]^T, \quad (2)$$

$$\mathbf{b}(\theta) = \frac{1}{\sqrt{N_r}}[1, e^{-j\pi\cos\theta}, \cdots, e^{-j\pi(N_r-1)\cos\theta}]^T, \quad (3)$$

where a half-wavelength antenna spacing for the ULA is assumed, and $\theta \in (0, \pi)$. Here, we emphasize that $\mathbf{a}(\theta)$ depends on $N_{t,n}$, which indicates that its size may change at different epoches. The beamforming vector $\mathbf{f}_n$ is designed by exploiting the predictive results as

$$\mathbf{f}_n = \mathbf{a}(\widehat{\phi}_{n|n-1}), \quad (4)$$

where $\widehat{\phi}_{n|n-1}$ denotes the predicted angle of CR at the nth epoch. Throughout this paper, we aim to predict and track the angle ϕ_n of the CR, so as to align the beam accurately and guarantee a reliable communication performance.

2.2. Radar Measurement Model

First, we aim to determine the resolved distances and velocities in the delay-Doppler domain by following a standard matched-filtering technique [2]. Then the refined output is expressed as

$$\widetilde{\mathbf{r}}_n = \kappa_n \sqrt{p_n}\sqrt{G}\sum_{k=1}^{K}\beta_{k,n}\mathbf{b}(\theta_{k,n})\mathbf{a}^H(\theta_{k,n})\,\mathbf{a}(\widehat{\phi}_{n|n-1}) \times \delta(\tau - \tau_{k,n}; \mu - \mu_{k,n}) + \widetilde{\mathbf{z}}_r, \quad (5)$$

where $\delta(\tau;\mu)$ is the normalized matched-filtering output function obtained by time and frequency-reversing and conjugating its own waveform for the complex transmit signal $s_n(t)$ [11]. Notice that $\delta(\tau;\mu)$ generally has a narrow-mainlobe property in both time domain and Doppler domain to ensure high distance and velocity resolution. The usage of matched-filter enables the receive signal-to-noise-ratio (SNR) of sensing to improve by a matched-filtering gain denoted as G. Note that G is equal to the number of symbols used for matched-filtering in a block. Besides, $\widetilde{\mathbf{z}}_n$ represents the noise output of matched-filtering. Hence, the distance and Doppler of the kth scatterer can be readily measured by finding the location of the corresponding peak position, expressed as

$$\widehat{\tau}_{k,n} = \frac{2d_{k,n}}{c} + z_{\tau_{k,n}}, \quad (6)$$

$$\widehat{\mu}_{k,n} = \frac{2v_n\cos(\theta_{k,n})f_c}{c} + z_{\mu_{k,n}}. \quad (7)$$

For the kth scatterer, substituting $t = \widehat{\tau}_{k,n}$ and $\mu = \widehat{\mu}_{k,n}$ into the matched-filtering output (5) yields

$$\widetilde{\mathbf{r}}_{k,n} = \kappa_n\beta_{k,n}\mathbf{b}(\theta_{k,n})\,\mathbf{a}^H(\theta_{k,n})\mathbf{a}(\widehat{\phi}_{n|n-1}) + \widetilde{\mathbf{z}}_r, \quad (8)$$

which indicates that K scatterers are totally separated. Here, $\widetilde{\mathbf{z}}_r$ denotes the measurement noise normalized by the transmit power p_n and the matched-filtering gain G, which follows $\widetilde{\mathbf{z}}_r \sim \mathcal{CN}(\mathbf{0}_{N_r}, \sigma_\theta^2\mathbf{I}_{N_r})$, where $\sigma_\theta^2 = \frac{\sigma^2}{Gp_n}$. Besides, the reflection coefficient $\beta_{k,n}$ is determined by the signal propagation distance and the RCS of the vehicle, expressed as

$$\beta_{k,n} = \frac{\varepsilon_{k,n}}{(2d_{k,n})^2} = \frac{\varepsilon_{k,n}}{c^2\tau_{k,n}^2}, \quad (9)$$

where $\varepsilon_{k,n}$ denotes the complex RCS of the kth slowly fluctuated Swerling I-type scatterer [12] at the nth epoch. The above thorough separation among scatterers is on the basis of the assumption that the sidelobe of $\delta(t)$ is negligible. In practice, sidelobes would affect the perfect separation and its influence is not considered in this article. Then $\theta_{k,n}$ can be readily measured by the maximum likelihood estimation (MLE) or the superresolution algorithms like multiple signal classification [13], whose measurement is expressed as

$$\widehat{\theta}_{k,n} = \theta_{k,n} + z_{\theta_{k,n}}. \quad (10)$$

Note that $z_{\theta_{k,n}}$, $z_{\tau_{k,n}}$ and $z_{\mu_{k,n}}$ are additive noises with zero means and variances of $\sigma_{k,n}^2(1)$, $\sigma_{k,n}^2(2)$ and $\sigma_{k,n}^2(3)$, respectively. Moreover, we remark here that the variances of the measurement noises are inversely proportional to the receive SNR of (5), i.e.,

$$\sigma_{k,n}^2(i) = \frac{a_i^2\sigma^2}{p_nG|\kappa_n\beta_{k,n}|^2\,|\delta_{k,n}|^2}, \; i = 1, 2, 3. \quad (11)$$

where $\delta_{k,n} = \mathbf{a}^H(\theta_{k,n})\mathbf{a}(\widehat{\phi}_{n|n-1})$ represents the beamforming gain factor of kth scatterer, whose modulus is less than 1 since the beam points to the CR rather than the kth scatterer. Finally, a_i, $i = 1, 2, 3$ are constants related to the system configuration, signal designs as well as the specific signal processing algorithms [2].

Now, with the measured $\widehat{\tau}_{k,n}$ and $\widehat{\theta}_{k,n}$, the coordinates of vehicle centroid (x_n, y_n) can be localized in the 2D Cartesian coordinate as

$$\widehat{x}_n = \frac{1}{K}\sum_{k=1}^{K} c\widehat{\tau}_{k,n}\cos\widehat{\theta}_{k,n}/2 = \frac{1}{K}\sum_{k=1}^{K}\widehat{d}_{k,n}\cos\widehat{\theta}_{k,n}, \quad (12)$$

$$\widehat{y}_n = \frac{1}{K}\sum_{k=1}^{K} c\widehat{\tau}_{k,n}\sin\widehat{\theta}_{k,n}/2 = \frac{1}{K}\sum_{k=1}^{K}\widehat{d}_{k,n}\sin\widehat{\theta}_{k,n}. \quad (13)$$

Now we estimate the velocity. Given that

$$\widehat{\mu}_{k,n} = \frac{2v_n\cos(\theta_{k,n})f_c}{c} + z_{\mu_{k,n}},\ \forall k \quad (14)$$

we reformulate K equations with the matrix-vector form as

$$\widehat{\boldsymbol{\mu}}_n = \mathbf{A}(\boldsymbol{\theta}_n)v_n + \mathbf{z}_\mu, \quad (15)$$

where $\mathbf{A}(\boldsymbol{\theta}_n) = [\frac{2f_c\cos(\theta_{1,n})}{c}, \cdots, \frac{2f_c\cos(\theta_{K,n})}{c}]^T$, $\widehat{\boldsymbol{\mu}}_n = [\widehat{\mu}_{1,n}, \cdots, \widehat{\mu}_{K,n}]^T$ and $\mathbf{z}_\mu = [z_{\mu_{1,n}}, \cdots, z_{\mu_{K,n}}]^T$.

It is straightforward to see that $\widehat{\boldsymbol{\mu}}_n \sim \mathcal{N}(\mathbf{A}(\boldsymbol{\theta}_n)v_n, \mathbf{Q}_\mu)$, where $\mathbf{Q}_\mu = \text{diag}(\sigma^2_{1,n}(3), \cdots, \sigma^2_{K,n}(3))$. In view of this, the MLE of v_n conditional to $\boldsymbol{\theta}_n$ is thus given as [14]

$$\begin{aligned}\widehat{v}_{n|\boldsymbol{\theta}_n} &= (\mathbf{A}^T(\boldsymbol{\theta}_n)\mathbf{Q}_\mu^{-1}\mathbf{A}(\boldsymbol{\theta}_n))^{-1}\mathbf{A}^T(\boldsymbol{\theta}_n)\mathbf{Q}_\mu^{-1}\widehat{\boldsymbol{\mu}}_n \\ &= \frac{c}{2f_c}\cdot\frac{\sum_{k=1}^{K}\widehat{\mu}_{k,n}\cos(\theta_{k,n})/\sigma^2_{k,n}(3)}{\sum_{k=1}^{K}\cos^2(\theta_{k,n})/\sigma^2_{k,n}(3)}.\end{aligned} \quad (16)$$

Since the relative position of the CR to the centroid can be known in advance, coordinates of the CR is thus $(x_n + \Delta x, y_n + \Delta y)$ when the antenna array is parallel to the road. Here, Δx and Δy are known according to the vehicle model. Finally, the measurement model is formulated as[1]

$$\begin{cases}\widehat{\phi}_n = \tan^{-1}\left(\dfrac{\widehat{y}_n + \Delta y}{\widehat{x}_n + \Delta x}\right) = \phi_n + z_\phi, \\ \widehat{d}_n = \sqrt{(\widehat{x}_n + \Delta x)^2 + (\widehat{y}_n + \Delta y)^2} = d_n + z_d, \\ \widehat{v}_n = \dfrac{c}{2f_c}\cdot\dfrac{\sum_{k=1}^{K}\widehat{\mu}_{k,n}\cos(\widehat{\theta}_{k,n})/\sigma^2_{k,n}(3)}{\sum_{k=1}^{K}\cos^2(\widehat{\theta}_{k,n})/\sigma^2_{k,n}(3)} = v_n + z_v,\end{cases} \quad (17)$$

where z_ϕ, z_d and z_v are measurement noises with zero means and variances of σ^2_ϕ, σ^2_d and σ^2_v, respectively. In practice, these variances are unknown. Here, we can use the first-order Taylor expansion to approximate them. The detailed derivations are omitted due to the space limitation.

2.3. Communication Receiver Model

A single receive antenna is deployed in the CR. We emphasize that, ISAC signal is used for both vehicle tracking and communication transmission during the entire frame structure. Hence, at the nth epoch, the vehicle receives the signal transmitted by the RSU as

$$y_n^C(t) = \alpha_n\kappa_n^C\sqrt{p}\mathbf{a}^H(\phi_n)\mathbf{a}_n(\widehat{\phi}_{n|n-1})s_n(t) + z_n^C(t), \quad (18)$$

where $\kappa_n^C = \sqrt{N_{t,n}}$ is the array gain. Besides, α_n indicates the Line of Sight (LoS) channel coefficient, which is given as [15]

$$\alpha_n = \alpha_{\text{ref}}d_n^{-1}e^{j\frac{2\pi f_c}{c}d_n}, \quad (19)$$

where $\alpha_{\text{ref}}d_n^{-1}$ denotes the LoS path-loss, and α_{ref} is a known reference path-loss measured at the distance of 1m.

The SNR of the CR is therefore given as

$$\text{SNR}_n^C = p_n\left|\kappa_n^C\alpha_n\right|^2\left|\bar{\delta}_{k,n}\right|^2/\sigma_C^2, \quad (20)$$

where $\bar{\delta}_{k,n} = \mathbf{a}^H(\phi_n)\mathbf{a}_n(\widehat{\phi}_{n|n-1})$ represents the beamforming gain factor, whose modulus equals to 1 if the predicted angle perfectly matches the real angle, and is less than 1 otherwise. Clearly, the angle prediction accuracy of CR plays a dominated role in the achievable rate of the vehicle. The achievable rate at the nth epoch is thus formulated as

$$R_n = \log(1 + \text{SNR}_n^C). \quad (21)$$

3. ISAC-BASED BEAM TRACKING SCHEME

Regarding the presentation of beamwidth, we refer readers to [16]. Here, instead of the first null beamwidth, we resort to the commonly-used half-power beamwidth for the ULA as $\theta_{BW} \approx \frac{1.78}{N_t\sin(\phi)}$. The coverage width Δd can thus be approximately calculated by a trigonometric function as $\Delta d \approx 2d\cdot\tan\left(\frac{0.89}{N_t\sin(\phi)}\right)$. Moreover, since the beamwidth varies at different epoches, the number of transmit antennas is calculated based on the predicted $\widehat{d}_{n|n-1}$ and $\widehat{\phi}_{n|n-1}$. Besides, we emphasize that the ISAC system allow a maximum antenna number as $N_{t,\max}$ (e.g., $N_{t,\max} = 128$). On the whole, the number of transmit antennas is given as

$$N_{t,n} = \min\left\{\left\lfloor\frac{0.89}{\arctan^{-1}\left(\frac{\Delta d}{2\widehat{d}_{n|n-1}}\right)\cdot\sin(\widehat{\phi}_{n|n-1})}\right\rfloor, N_{t,\max}\right\}. \quad (22)$$

At the nth epoch, the state vector is composed of the angle, the distance and the velocity of CR, given as $\mathbf{x}_n = (\phi_n, d_n, v_n)^T$. Following the derivation in [2], it is straightforward to summarize the state evolution model of CR as

$$\begin{cases}\phi_n = \phi_{n-1} + d_{n-1}^{-1}v_{n-1}\Delta T\sin(\phi_{n-1}) + \omega_\phi, \\ d_n = d_{n-1} - v_{n-1}\Delta T\cos(\phi_{n-1}) + \omega_d, \\ v_n = v_{n-1} + \omega_v.\end{cases} \quad (23)$$

[1]Note that $\arctan^{-1}(x) \in (-\pi/2, \pi/2)$, while the angle of vehicle is defined in the region of $[0, \pi)$. For clarity, we define $\tan^{-1}(x) = \arctan(x)$ if $x \geq 0$, otherwise $\tan^{-1}(x) = \arctan(x) + \pi$.

Table 1. Parameters in Simulations.

Parameter	Value	Parameter	Value	Parameter	Value
T	$6.0s$	ΔT	$0.01s$	f_c	30GHz
p	1	Δd	$6m$	v	$20m/s$
Δx	$1.5m$	Δy	$0.5m$	α_{ref}	1
$N_{t,\max}$	128	a_1	$1.05e^{-2}$	a_2	$3.5e^{-2}$
a_3	$1.05e^{-2}$	N_r	128	K	8
$\bar{\sigma}_\phi$	0.01°	$\bar{\sigma}_d$	$0.1m$	$\bar{\sigma}_v$	$0.25m/s$
σ^2	0.15	σ_C^2	1	G	10

The state evolution model and the measurement model are reformulated by more compact matrix-vector forms as

$$\begin{cases} \text{State Evolution Model: } \mathbf{x}_n = \mathbf{h}(\mathbf{x}_{n-1}) + \boldsymbol{\omega}_n, \\ \text{Measurement Model: } \mathbf{y}_n = \mathbf{x}_n + \mathbf{z}_n, \end{cases} \tag{24}$$

where $\mathbf{y}_n = \widehat{\mathbf{x}}_n = [\widehat{\phi}_n, \widehat{d}_n, \widehat{v}_n]^T$, $\boldsymbol{\omega}_n = [\omega_\phi, \omega_d, \omega_v]^T$, and $\mathbf{z}_n = [z_\phi, z_d, z_v]^T$. As considered above, both $\boldsymbol{\omega}_n$ and $\mathbf{z}_n$ are zero-mean Gaussian distributed, with covariance matrices being expressed as

$$\mathbf{Q}_w = \text{diag}(\bar{\sigma}_\phi^2, \bar{\sigma}_d^2, \bar{\sigma}_v^2), \tag{25}$$

$$\mathbf{Q}_z = \text{diag}(\sigma_\phi^2, \sigma_d^2, \sigma_v^2). \tag{26}$$

In terms of the non-linearity of the state evolution model, the standard Kalman filtering cannot be directly utilized. Therefore, EKF is used by linearizing the state evolution model, where the Jacobian matrix should be derived, given as

$$\mathbf{H} = \frac{\partial \mathbf{h}}{\partial \mathbf{x}} = \begin{bmatrix} 1 + \frac{v\Delta T \cos(\phi)}{d} & -\frac{v\Delta T \sin(\phi)}{d^2} & 0 \\ v\Delta T \sin(\phi) & 1 & -\Delta T \cos(\phi) \\ 0 & 0 & 1 \end{bmatrix}. \tag{27}$$

Following the standard procedure of EKF [14], the state prediction and tracking can be achieved. To save the space, the EKF procedure is omitted.

4. SIMULATIONS

If not otherwise specified, simulative parameters are listed in Table. 1. Beyond that, we assume that coordinates of the RSU are $(0m, 0m)$, and the initial position of the vehicle is $(60m, 20m)$. In simulations, we model the vehicle with eight resolved scatterers uniformly distributed in the rectangle. Besides, the vehicle moves in the direction of the negative x-axis.

In Fig. 2, it is shown that $N_{t,n}$ reduces when the vehicle approaches the RSU. The reason is because covering the entire vehicle at this moment requires a wider beamwidth. Besides, we also provide the result of $|\alpha_n \kappa_n^C|^2$ versus time. Clearly, when approaching the RSU, $|\alpha_n|^2$ increases due to the closer distance, while $|\kappa_n^C|^2$ degrades in terms of the smaller $N_{t,n}$. The results indicate that the number of array antenna plays a more dominated role in the receive SNR.

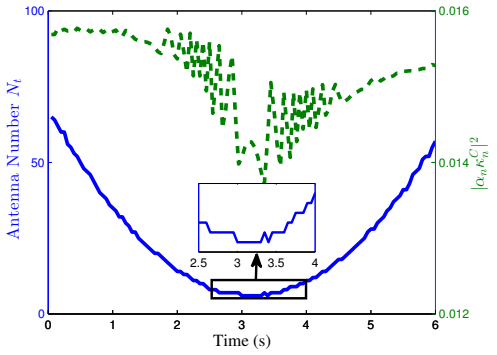

Fig. 2. $N_{t,n}$ versus time and $|\alpha_n \kappa_n^C|^2$ versus time.

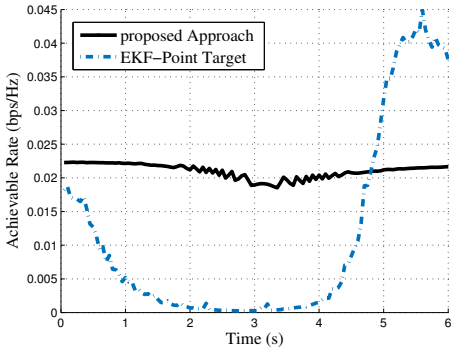

Fig. 3. Achievable rate versus time: the proposed approach and EKF-point target approach.

In Fig. 3, we compare the proposed approach with the EKF-based beam tracking for point targets [2]. For the latter, the antenna number is fixed at $N_t = 128$, and we randomly select a scatterer to be tracked. Overall, the proposed approach achieves a relatively stable communication performance, and is superior to EKF-point target in most epoches. When the vehicle approaches the RSU, the narrow beam of EKF-point target cannot cover the scatterer and the CR simultaneously, arising a significant performance loss. When the vehicle drives away, the scatterer and the CR can be covered and EKF-point target may have the higher rate than the proposed approach at price of the much higher array gain.

5. CONCLUSION

In this paper, we have proposed an ISAC-based predictive beam tracking approach in V2I networks for the extended target vehicle. The main idea is to dynamically adjust the beamwidth according to the prediction information, so as to illuminate the entire vehicle and infer the position of the CR in terms of resolved scatterers. Numerical results have validate the effectiveness of the proposed scheme over the previous EKF-based beam tracking for point targets in [2].

6. REFERENCES

[1] H. Wymeersch, G. Seco-Granados, G. Destino, D. Dardari, and F. Tufvesson, "5G mmwave positioning for vehicular networks," *IEEE Wireless Commun*, vol. 24, no. 6, pp. 80–86, 2017.

[2] F. Liu, W. Yuan, C. Masouros, and J. Yuan, "Radar-assisted predictive beamforming for vehicular links: Communication served by sensing," *IEEE Trans. Wireless Commun*, vol. 19, no. 11, pp. 7704–7719, 2020.

[3] W. Yuan, F. Liu, C. Masouros, J. Yuan, D. Wing Kwan Ng, and N. González-Prelcic, "Bayesian predictive beamforming for vehicular networks: A low-overhead joint radar-communication approach," *IEEE Trans. Wireless Commun*, vol. 20, no. 3, pp. 1442–1456, 2020.

[4] J. Wang, Z. Lan, C.-woo Pyo, T. Baykas, C.-sean Sum, M. A. Rahman, J. Gao, R. Funada, F. Kojima, and H. Harada, "Beam codebook based beamforming protocol for multi-Gbps millimeter-wave WPAN systems," *IEEE J. Sel Areas. Commun*, vol. 27, no. 8, pp. 1390–1399, 2009.

[5] D. Zhang, A. Li, M. Shirvanimoghaddam, P. Cheng, Y. Li, and B. Vucetic, "Codebook-based training beam sequence design for millimeter-wave tracking systems," *IEEE Trans. Wireless Commun*, vol. 18, no. 11, pp. 5333–5349, 2019.

[6] D. Zhu, J. Choi, and R. W. Heath, "Auxiliary beam pair enabled AoD and AoA estimation in closed-loop large-scale millimeter-wave MIMO systems," *IEEE Trans. Wireless Commun*, vol. 16, no. 7, pp. 4770–4785, 2017.

[7] F. Liu, P. Zhao, and Z. Wang, "EKF-based beam tracking for mmwave MIMO systems," *IEEE Commun. Lett*, vol. 23, no. 12, pp. 2390–2393, 2019.

[8] F. Liu, Y. Cui, C. Masouros, J. Xu, T. X. Han, Y. C. Eldar, and S. Buzzi, "Integrated sensing and communications: Towards dual-functional wireless networks for 6G and beyond," *arXiv preprint arXiv:2108.07165*, 2021.

[9] Y. Cui, F. Liu, X. Jing, and J. Mu, "Integrating sensing and communications for ubiquitous IoT: Applications, trends and challenges," *IEEE Network*, vol. 35, no. 5, pp. 158–167, 2021.

[10] F. Liu and C. Masouros, "A tutorial on joint radar and communication transmission for vehicular networks-part iii: Predictive beamforming without state models," *IEEE Commun. Lett*, 2020.

[11] W. Yi, T. Zhou, Y. Ai, and R. S. Blum, "Suboptimal low complexity joint multi-target detection and localization for non-coherent MIMO radar with widely separated antennas," *IEEE Trans. Signal Process*, vol. 68, pp. 901–916, 2020.

[12] M. A. Richards, *Fundamentals of radar signal processing*, McGraw-Hill Education, 2014.

[13] M. Keskin, H. Wymeersch, and V. Koivunen, "ICI-aware parameter estimation for MIMO-OFDM radar via APES spatial filtering," in *ICASSP 2021-2021 IEEE International Conference on Acoustics, Speech and Signal Processing (ICASSP)*. IEEE, 2021, pp. 8248–8252.

[14] S. Kay, *Fundamentals of Statistical Signal Processing, Vol. I: Estimation Theory*, Upper Saddle River, NJ: Prentice-Hall PTR, 1993.

[15] L. Liu, S. Zhang, and R. Zhang, "CoMP in the sky: UAV placement and movement optimization for multi-user communications," *IEEE Trans. Commun*, vol. 67, no. 8, pp. 5645–5658, 2019.

[16] H. L. Van Trees, *Optimum array processing: Part IV of detection, estimation, and modulation theory*, John Wiley & Sons, 2004.